A multimodal, implantable sensor array and measurement system to investigate the suppression of focal epileptic seizure using hypothermia

B. Csernyus[1*], Á. Szabó[1,2*], R. Fiáth[1,3], A. Zátonyi[1], C. Lázár[4], A. Pongrácz[1], Z. Fekete[1]

1 Research Group for Implantable Microsystems, Faculty of Information Technology & Bionics, Pázmány Péter Catholic University, Hungary

2 Roska Tamás Interdisciplinary Doctoral School, Pázmány Péter Catholic University, Hungary

3 Institute of Cognitive Neuroscience & Psychology, Research Centre for Natural Sciences, Hungary

4 Microsystems Laboratory, Institute of Technical Physics & Material Sciences, Center for Energy Research, Hungary

* Authors equally contributed.

Abstract

Objective. Local cooling of the brain as a therapeutic intervention is a promising alternative for patients with epilepsy who do not respond to medication. *In vitro* and *in vivo* studies have demonstrated the seizure-suppressing effect of local cooling in various animal models. In our work, focal brain cooling in a bicuculline induced epilepsy model in rats is demonstrated and evaluated using a multimodal micro-electrocorticography (microECoG) device.

Approach. We designed and experimentally tested a novel polyimide-based sensor array capable of recording microECoG and temperature signals concurrently from the cortical surface of rats. The effect of cortical cooling after seizure onset was evaluated using 32 electrophysiological sites and 8 temperature sensing elements covering the brain hemisphere, where injection of the epileptic drug was performed. The focal cooling of the cortex right above the injection site was accomplished using a miniaturized Peltier chip combined with a heat pipe to transfer heat. Control of cooling and collection of sensor data was provided by a custom designed Arduino based electronic board. We tested the experimental setup using an agar gel model *in vitro*, and then *in vivo* in Wistar rats.

Main results. Spatial variation of temperature during the Peltier controlled cooling was evaluated through calibrated, on-chip platinum temperature sensors. We found that frequency of epileptic discharges was not substantially reduced by cooling the cortical surface to 30 °C, but was suppressed efficiently at temperature values around 20 °C. The multimodal array revealed that seizure-like ictal events far from the focus and not exposed to high drop in temperature can be also inhibited at an extent like the directly cooled area.

Significance. Our results imply that not only the absolute drop in temperature determines the efficacy of seizure suppression, and distant cortical areas not directly cooled can be influenced.

Keywords: hypothermia; seizure suppression; Peltier-device; epilepsy; brain cooling; microECoG

Highlights

1. A novel sensor array was microfabricated capable of recording electrical and thermal signals simultaneously. The size and shape of the flexible polyimide-based electrode can be tailored to specific applications depending on the target area size.
2. The effect of cooling on focally induced epilepsy was investigated in a rat model.
3. Spatial and temporal microECoG data could be correlated with brain surface temperature induced by Peltier cooling.
4. We observed that the rate and amplitude of epileptiform spikes diminished not only underneath the Peltier cell, but also in the surrounding tissue suggesting that the effects of local hypothermia can spread beyond the area directly affected by cooling.

1. Introduction

Epilepsy is a heterogeneous group of chronic neurological disorders that are characterized by recurrent unprovoked seizures. Epileptic seizures occur when neurons are intermittently activated in an abnormally excessive and highly synchronous manner [1]. Focal and generalized seizures are distinguished according to the localization of activated neurons. The onset of a focal

seizure is limited to a part of one cerebral hemisphere, during generalized seizures, the initial activation of neurons happens throughout both hemispheres [2]. Interictal epileptiform activity can also occur in epilepsy patients, taking the form of epileptiform discharges (EDs), which are simply transients with a characteristic spiky morphology. EDs are important in the diagnosis of epilepsy [3].

Primarily, epilepsy is treated with the administration of antiepileptic drugs (AEDs), but even the best medications cannot control the seizures of over 30% of epilepsy patients [4]. These patients are considered to have refractory epilepsy [5]. In these cases, surgical resection can only be performed if the epileptogenic foci are not located in eloquent areas such as the motor and speech cortices, and it is not always successful [6]. An alternative to surgery would be the application of focal brain cooling. Numerous animal studies show the efficacy of focal cooling in terminating ongoing seizures, reducing seizure frequency and the amplitude of epileptic discharges [7]. Human trials with the use of therapeutic hypothermia were also conducted, investigating its beneficial effects on other disorders as well, such as traumatic brain injury [8] or ischemic stroke [9].

There are several possible mechanisms suggested by which focal cooling exerts its antiepileptic effects, however, the exact mechanisms are poorly characterized. Some of the mechanisms are a reduction in neurotransmitter release, alternation of activation-inactivation kinetics in voltage-gated ion channels and slowing of catabolic processes [6].

There has been a good number of different techniques and approaches to achieve local hypothermia to mitigate the symptoms of epilepsy. Irrigating the exposed brain surface with ice cold saline is a widespread method used by neurosurgeons during operations [10,11]. Operative neurosurgical mapping potentially induces focal seizure activity that can be rapidly halted by irrigating the brain surface with cold Ringer's solution [12,13].

Passive focal cooling is also feasible using heat dissipation elements such as a metal plate placed in contact with the brain surface [14]. It only produces a slight (1-2 °C) and uncontrolled temperature reduction. Though this degree of cooling proved to be adequate to inhibit epileptic seizures [14], a drawback of passive focal cooling is that it cannot differentiate between normal and epileptic brain states, preventing targeted intervention.

Active focal cooling devices can use some sort of liquid as their cooling medium. In most cases, a metal tubing shaped as a loop or a coil serves as the cooling surface through which chilled saline, ethanol or methanol is circulated [15,16]. Size and shape of tubing can be tailored to any specific use such as surface or deeper cooling of sulci [17].

In our case, a Peltier device was utilized for local cooling, which is a widely used tool in animal studies to induce hypothermia in a specific area of the brain [18–20]. Peltier cells are a series of semiconductors sandwiched between two ceramic plates and they can vary in size from a few millimeters to several centimeters making them applicable to cooling brain surfaces of small animals as well as humans. A Peltier chip utilizes the thermoelectric effect, one side of it rapidly cools, while the other heats up when current is passed through it. A Peltier chip is also suitable for cooling deeper structures, such as the hippocampus [21] by attaching a needle to its cold side. Besides the opportunities to use such devices for brain hypothermia, there have been no efforts to characterize the effective cross-section of such intervention in terms of temperature distribution or electrophysiological response.

In this paper, we report on the design and implementation of a multimodal sensor array along with a Peltier-based cooling system. The objective was to record electrophysiological and temperature data from the rat cortex, and the effectiveness of Peltier cooling was tested in suppressing epileptic activity induced by local injection of bicuculline.

2. Methods

2.1 Design of experiment

Our work aimed at the experimental testing of the flexible cortical sensor grid in combination with thermoelectric cooling in anesthetized rats. The objective of the *in vivo* experiment was 1) to record micro-electrocorticography (microECoG) and temperature data from the cortex of rats during anesthesia thereby confirming the functionality of the probe and recording setup and 2) to test the efficacy of focal cooling in decreasing experimentally induced epileptic activities.

An overview of microEcoG device layout and dimensions is presented on Figure 1. 32 recording sites in a 4 x 8 configuration are used to record electroencephalography (EEG) signals from the exposed brain surface. An aperture with a diameter of 0.8 mm in the middle line is used to locate intracortical injection of bicuculline. Eight temperature sensor filaments (Figure 1b) are positioned in between recording sites (Figure 1c) in a 3-2-3 configuration around the injection site. The sensor grid was connected to the Arduino-controlled board, which was connected to a PC through a USB port to capture the temperature data. Electrophysiological signals were recorded using an INTAN pre-amplifier (Part #C3314, INTAN Technologies, USA) at a sampling rate of 20

kHz. Before and after cooling down the cortical surface, baseline neural activity was recorded. To evoke seizure-like activity, bicuculline was injected into the cortex through the hole in the center of the grid. The Peltier device was placed carefully on the top of the sensor grid. Upon the emergence of epileptiform activity cooling current was applied to the Peltier chip. The Peltier device mounted to a heat pipe was powered by a source meter unit. The electric current to cool down the side of the Peltier chip in contact with the brain tissue was adjusted between 0.1 A and 1 A. More technical details on device fabrication and testing are summarized in the following sections.

2.2 Fabrication of the multimodal microarray

To perform our measurements, polyimide based microECoG device was realized, which have been demonstrated outstanding in vivo and in vitro performance [22–25]. Recording sites, sensor filaments and wires are patterned in the same conductive layer (platinum). The 10 µm thick flexible microECoG device was fabricated at the clean room of the University of Freiburg relying on established processes that have already tested elsewhere [26]. 150 mm (6”) silicon wafers were cleaned with HF dip and 5µm thick polyimide (UBE UPIA-ST1001, UBE Industries Ltd., Japan) was spin-coated and annealed. A lift-off pattern consisting of AZ9260 and AZ5214E (Microchemicals GmbH, Germany) photoresist was formed, and a conductive layer of 250 nm platinum sandwiched between two layers of 25 nm titanium was evaporated. After performing the lift-off process in DMSO (dimethyl-sulfoxide), a second layer of 5-µm-thick polyimide was spin-coated on top of the patterned conductive layer. A second photolithography step relying on AZ9260 photoresist was applied to define the outline and recording sites of the device. Reactive ion etching in CF_4/O_2 plasma was used to complete the release of the polyimide substrate. The top layer of titanium on the recording sites is removed in HF to expose the platinum surface. The final layer composition at two different cross-sections of the layout is shown in Figure 1d. An Omnetics connector (A79022-001, Omnetics Connector Corporation, USA) was attached to the connector end for signal readouts. The interconnection between the platinum surface and the connector pins was formed using a conductive epoxy (CW2400, Chemtronics, USA). After cross-linking, the interconnections were covered with another insulation layer of epoxy (Araldite, Hunstman Corp., USA) to maintain mechanical and electrical stability of the device backbone. The ready-to-use multimodal microECoG device is presented in Figure 1e-f.

2.3 Electrochemical characterization

Prior to *in vivo* measurement, long term electrochemical stability of the proposed combination of materials was tested. The array was immersed in 0.01 M phosphate buffered saline (PBS tablet diluted in 200 mL distilled water yielding 0.01 M phosphate buffer, 0.0027 M potassium chloride and 0.137 M sodium chloride, pH 7.4, at 25 °C, Merck KGaA, Germany solution) for 22 days. Electrochemical impedance spectroscopy (EIS) was performed during the period of electrochemical stability experiment using a Gamry Reference 600+ Potentiostat (Gamry Instruments, *Warminster, PA, US*) using 25 mV rms and frequency range from 1 Hz to 10 kHz. A leakless miniature Ag/AgCl electrode (ET072-1, eDAQ Pty Ltd., Australia), a platinum wire and the microECoG sites were used as reference, counter and working electrodes, respectively. The array was submerged in PBS up to the Omnetics connector.

2.4 Peltier based cooling system to produce cortical hypothermia

To induce hypothermia to the cortical surface, we used a small 2.5 x 2.5 x 1.4 mm Peltier module (type: 00801-9B30-10RU3, Qcmax = 0.58 W, Imax = 1 A, Umax = 1 V, Custom Thermoelectric LLC, USA). During operation, the current passing through the device cools one side, while heating up the other side of it, due to the thermoelectric effect. A sintered copper heat pipe (QuickCool QY-SHP-D3-200SA, Conrad Electronic GmbH, Germany) with 3 mm diameter and 200 mm length was used to dissipate heat from the hot side of the Peltier module. To increase the contact surface between the Peltier module and the heat pipe, an additional copper block was soldered to the end of the heat pipe, and the Peltier was glued to the block using Arctic Silver epoxy-based heat conducting glue made from a 1:1 ratio mixture of its components. The outlets of the Peltier were connected to a DC power supply (PS-302A, Kusam Electrical Industries Ltd, India) to control the cooling current. Using a maximum current strength of 1 A the exposed side of the Peltier quickly cools, while the excess heat is dissipated by the heat pipe through the copper block.

2.5 Calibration of sensors & thermal actuator

The 8 resistive temperature sensors on the microECoG needed to be calibrated before they were used for temperature measurement. The calibration range was from 40 °C down to 5 °C. An aluminum cylinder was filled up with warmed water and put in a water bath, which we cooled down gradually using ice. We placed a K-type nickel chromium-nickel silicon thermometer connected to a multimeter (TENMA 72-7730A, Tenma Corporation, Japan) and the microECoG in the cylinder.

Recording from the temperature sensors during both calibrations and *in vivo* tests was based on a measurement scheme shown in Supplementary Figure S1. Temperature measurement from the microECoG was carried out using resistive temperature sensors in a four-lead arrangement. An Arduino Due R3 (Arduino Corporation, Italy) unit was responsible for controlling the measurement. Three 32 channel ADG731 analogue multiplexer/demultiplexer units (Analog Devices Inc., USA) switch among the different temperature sensors. One switches the feed current generator, the other two switch the output voltage to the amplifier. Grounding is shared by all the units. Output voltage is amplified by a INA326 instrumentation amplifier (Texas Instruments, USA), then a ADS1252 delta-sigma A/D converter (Texas Instruments, USA) provides the recordable digital signal. The sampling rate was set to 100 Hz. Each sensor is measured multiple times in quick succession to reduce measurement noise. The system calculates the average value and transfers that to the computer.

We read the temperature values from the multimeter every 5 °C and paired that with current measurement data from the microECoG. The computer displayed readings from the thermal contacts in raw counts, which could be converted to resistance using the known parameters of gain, reference voltage, and the measuring current for each contact. Calculated resistance values were plotted against measured temperature and a linear fit gave the calibration equation for each contact.

To investigate the degree of cooling in relation to the driving current applied to the Peltier cell, we used an *in vitro* agar gel model. A roughly cube shaped piece of agar served to mimic the brain surface with the microECoG and the Peltier chip placed on top of it. Except for the top surface, the agar gel was submerged in a tempered water bath kept at 45 °C, so the top of the gel was around 35-38 °C.

To understand how the degree of cooling decays with distance from the Peltier cell, we placed the cell on the microECoG surface in four different but overlapping positions. In each position three measurements were made using driving currents of 0.1 A, 0.25 A and 0.5 A.

Similarly, to the *in vivo* testing, the measurements consisted of periods before cooling, during cooling and after cooling. The length of these were 1 minute - 1 minute - 1 minute, 1 minute - 2 minutes - 1 minute and 1 minute - 2 minutes - 1.5 minutes for currents of 0.1 A, 0.25 A and 0.5 A, respectively.

2.6 Surgery & animal model of epilepsy

All experiments were performed according to the EC Council Directive of September 22, 2010 (2010/63/EU), and all procedures were reviewed and approved by the Animal Care Committee of the Research Centre for Natural Sciences and by the National Food Chain Safety Office of Hungary (license number: PE/EA/775-7/2020). Acute *in vivo* experiments were carried out on Wistar rats (n = 2; 180 g and 270 g; females). Animals were anesthetized with an intramuscularly administered mixture of ketamine (75 mg/kg of body weight) and xylazine (10 mg/kg of body weight). During the electrophysiological recordings, supplementary intramuscular injections of the ketamine/xylazine cocktail were given to maintain the deep anesthetic state. A homeothermic heating pad connected to a temperature controller (Supertech, Pécs, Hungary) was used to keep the body temperature of the rats at normothermia. After reaching the appropriate anesthetic depth for surgery, animals were placed in a stereotaxic frame (David Kopf Instruments, Tujunga, CA, USA). Next, we removed the skin and the connective tissue from the top of the skull, then a cranial window with a size of about 10 mm × 5 mm was drilled over the left brain hemisphere (anterior-posterior [AP]: from +1 mm to -9 mm; medial-lateral [ML]: from 0.5 mm to 5.5 mm [or until the lateral edge of the parietal and frontal bones was reached]; coordinates given with respect to the bregma[1]). The dura mater was left intact during the whole experiment. The microECoG array was mounted on a micromanipulator, then carefully lowered into the craniotomy and placed on the exposed cortical surface. To prevent dehydration of the brain tissue, room temperature physiological saline solution was regularly dropped into the cavity of the cranial window. A stainless-steel needle inserted in the nuchal muscle of the animal served as the reference and ground electrode during recordings. Cortical electrical activity was collected using an Intan RHD2000 electrophysiological recording system (Intan Technologies, Los Angeles, CA, USA) equipped with a 64-channel headstage. Wideband signals (0.1 – 7500 Hz) were acquired with 20 kHz/channel sampling rate and with 16-bit resolution. Electrophysiological data were saved to a local network attached storage device for offline analysis.

To induce epileptiform activity, bicuculline (1 mM, 10-20 µl) was injected into the brain using a 34-gauge needle. The needle attached to a Hamilton syringe was mounted on a micromanipulator, then slowly lowered to a cortical depth of 1.5 mm through the aperture of the microECoG array. Epileptiform spikes appeared a few minutes after bicuculline injection. After that, the injection needle was retracted, and the Peltier chip was placed on top of the microECoG array over the injection site.

2.7 Electrophysiology & data analysis

Electrophysiological signals were recorded after bicuculline injection both with and without cortical cooling. One minute control signal was measured before and after the cooling. The analysis was performed with a custom Matlab program. The raw data was pre-processed using a high-pass (1.5 Hz third-order Butterworth) a bandstop (50 Hz 20th-order IIR) and low-pass (100 Hz fifth-order Butterworth) filter. Turning on and off the Peltier cooling device also caused artifacts of large amplitude, which were removed from the dataset by a threshold. One recording contains three, separable parts: before, during and after cooling. To quantify any difference in spiking activity between the different temperature periods, a simple, threshold-based spike detection was implemented. Spike rate was defined as the reciprocal of the average time between the detected spikes in the given time window. We also calculated the average amplitude of spikes in a time window. During cooling, some measurements contained only a few epileptic form spikes, therefore a suitable overlapping window size was required to be able to compare the different periods of the measurement. For the statistical data and the represented figures, 30 s long time windows were used with 7.5 s overlapping (quarter of the window size). The visualized changes were calculated from the deviation from the initial value (spiking rate of the current window - spiking rate of the 1st window and same in case of average amplitude). The significance of cooling on spike rate and average amplitude was calculated with paired sample t-test with a 0.05 significance level.

3. Results

3.1 Long-term electrochemical performance

Long-term electrochemical performance of softening polymer based microECoG are presented in Figure 3a-c. Before *in vivo* measurement, the sites were soaked in 0.01 M PBS for 22 days. Impedance magnitude and phase of a representative device are shown in Figure 3a-b over the frequency range from 1 Hz to 10 kHz. Pale grey curves and pale blue curves represent the impedance and phase of single recording sites respectively, while bold lines represent the mean of impedance and phase of the 32 recording sites on the 1st (Figure 3a) and 22nd (Figure 3b) day of the electrochemical stability experiment. Average impedance values ± standard deviation at 1 kHz are shown in Figure 3c. Analyzing Bode plots, changes in phase angle between the frequency range from 1 Hz to 1 kHz can be observed when comparing the 1st and the 22nd day of the experiment. Slight alteration in impedance can be seen in Figure 3c. The initial 200 kOhm decreased then stabilized and remained stable at around 170 kOhm by the 7th day of the experiment and afterwards. The reduced impedance showed lower standard deviation over soaking time (Figure 3c) imply an enhancement approaching better electrophysiological recording quality. Decrease in impedance and increase in phase angle indicate a shift in charge transfer mechanism from a capacitive behavior to a faradaic or resistive behavior over time. This observation is similar to that Leber et al. presented in their work [27] and does not deteriorate microECoG performance after a steady state is reached.

3.2 Calibration results of thermal sensors and actuator

Figure 3d shows the calibration graph for the platinum temperature sensor contacts T1-T8. The graph shows the measured temperature of the K-type thermometer plotted against the calculated resistance values of the contacts. The contacts of the temperature sensor array were calibrated with a K-type thermometer in the range of 5 °C to 40 °C. The functions display adequate linearity within that temperature range with R^2 values at least 0.9962.

During calibration of the Peltier-based cooling system, we determined that the speed of heat-transfer from the heat-pipe towards the environment is getting limited above the current

value of 0.5 A, which results in unstable tissue temperature and a risk of temperature overshooting during OFF periods. For this reason, we did not take any attempt to approach the maximum driving current (I = 1 A) of the system. Figure 4 shows the change of temperature along the multimodal microECoG at five distances from the midline of the Peltier-chip. Based on the measurement with our platinum temperature sensor array, we proved that there is little change in temperature at the outline of the chip with respect to the core part (within 1 °C), however, there is a substantial drop in temperature values moving away from the chip. The initial values under the chip (green and black colored plots) are lower by approximately 1.5 °C compared to other sites, which is caused by the passive cooling effect of the Peltier-chip even though it is out of operation. These are important features to be considered during the evaluation of cooling induced variation in electrophysiology signals.

3.3 Effect of focal cooling on cortical activity after seizure onset

Cortical response to focal brain cooling has not been interrogated using a multifunctional microECoG device yet. The potential of our device in this field was demonstrated using three current values that controlled the Peltier chip (I = 0.1 A, 0.25 A, 0.5 A). Figure 5 shows the general effect of hypothermia in the raw data recorded via the 32-channel microECoG array. Frequency and amplitude of ictal activity recorded at the current value 0.1 A are less affected by the drop of 6-7 °C underneath the Peltier chip, however, in the other cases the possibility of spike generation is reduced.

It is important to note, that in our measurement scheme, we carefully place the Peltier chip on the exposed brain surface and avoid any extra pressure besides the inherent pressure caused by the chip weight. This weight however does not induce dimpling of the tissue, which may block the circulation of blood in the superficial layer of the brain. Regarding the recorded iEEG activity, there was no apparent change due to the presence of the Peltier chip.

Raw data from a representative channel located underneath the Peltier chip is presented in Figure 6 in response to a drop of (a) 6-7 °C (I = 0.1 A), (b) 12-13 °C (I = 0.25 A), (c) 20-21 °C (I = 0.5 A) after bicuculline injection. Using additional dose of bicuculline (Figure S2, S3), we maintained the cooling onset for 5 minutes to test the stability of the suppressing effect. To reach the maximum temperature drop, at least 10 seconds was necessary. In contrast, the suppression of spiking activity starts immediately as the Peltier-chip is switched on, which implies that the

affected cortical cells are also responsive to the temporal gradient in temperature, and reaching a particular threshold is not the only way to block their synchronized activity.

3.4 Frequency and amplitude of ictal spikes during cooling onset

Change in ictal spike frequency and amplitude is shown in Figure S2-S3. On recording sites underneath the Peltier chip, the decrease in spike rate is the highest. The extent of reduction in the frequency is higher at lower temperatures. The maximum change is approximately 7-fold and 5-fold in the cases of 0.5 and 0.25 A, respectively. Unlike spike rate, spike amplitude is affected only by lower temperatures. We observed no significant effect when using a driving current of 0.25. In the case of 0.5 A, spike amplitude significantly decreased. A paired-samples t-test was conducted to compare the spike rate and average amplitude before and during cooling. There was a significant difference in the scores for baseline spike rate ($M=3.71$, $SD=1.85$) and spike rate during cooling with 0.25 A ($M=1.69$, $SD=0.81$), $t(63) =10.20$, $p<0.001$. Similarly, significant difference was seen between baseline spike rate ($M=5.20$, $SD=2.08$) and spike rate during cooling with 0.5 A ($M=2.05$, $SD=0.97$), $t(63)=15.98$, $p<0.001$. In case of average amplitude there was no significant difference in case of 0.25 A cooling (baseline [$M=493.84$, $SD=73.14$], cooling [$M=479.43$, $SD=65.88$], $t(63)= 1.91$, $p=0.06$) however in case of 0.5 A cooling there was a significant difference (baseline [$M=517.45$, $SD=70.14$], cooling [$M=472.13$, $SD=58.96$], $t(63)=6.89$, $p<0.001$) . The boxplot in Figure 7 shows these data for a 5-minute-long cooling session, which proves that suppression is stable well beyond the initial transition of temperature. Interestingly, the epileptic activity measured at a remarkable distance from the chip was also mitigated, even though the decrease in temperature on these brain areas is much lower according to Figure 4. Moving away from the midline of the Peltier-chip by 2.5 mm results in a temperature drop of only 3 °C and 1.5 °C for 0.5 A and 0.25 A driving currents, respectively. As seen on Figure 6, this range should not contribute to any remarkable change in the epileptic activity.

4. Discussion

The cooling setup in this study consisted of a small Peltier device with a sintered copper heat pipe attached to it.

We observed a passive cooling effect of the Peltier cell before it was turned on: a 1.5 °C drop in surface temperature occurred underneath the device. Similar values were reported when using a metal plate as a passive cooling element, and that this slight reduction proved to be enough to suppress EDs [14]. We, however, did not observe that this passive cooling had any influence on the frequency and amplitude of spiking.

Both *in vitro* and *in vivo* testing showed that the Peltier cell produces great temperature reductions in a matter of seconds even at 0.5 A driving current, which is half of the maximal applicable current strength. Maximal temperature drops were 23 °C and 20-21 °C for *in vitro* and *in vivo* measurements, respectively. These resulted in surface temperatures below 15 °C, which is suggested to be a safety limit for seizure frequency and neurologic function improvement [28]. Cooling further to 10 °C can also suppress seizures, but with no further improvement in neurologic function [28]. Even these low temperature values will not cause any irreversible damage. To cause irreversible histological change and motor dysfunction, brain tissue has to be cooled to freezing point or below [29].

The extent of temperature reduction has a strong influence on the anticonvulsant effect of hypothermia [30], and termination of epileptic discharges could be caused by cooling-induced changes in the electrophysiological properties of neuronal membranes [31]. Our results show that epileptic spike frequency diminished 5-fold and 7-fold compared to precooling values for 0.25 A and 0.5 A driving currents, resulting in a 12-13 °C and 20-21 °C temperature drop, respectively. Cooling to this degree delays repolarization and broadens spike duration leading to a reduction in spike frequency thereby terminating epileptic discharges [31]. The 6-7 °C temperature reduction caused by the 0.1 A driving current barely affected frequency and amplitude of epileptic spikes. This coincides with the observation that cooling to at least 24 °C was needed to reduce seizures with a Peltier device *in vivo* in rats [32]. The same authors measured a reduction in seizure duration from 85.7 ± 26.2 seconds to 8.4 ± 5 seconds by cooling to 20-25 °C [33]. Also using Peltier to cool hippocampal slices, seizures were terminated in 8 seconds at 21 °C [34], and cooling to 20 °C completely suppressed epileptic activity *in vivo* in 40% of animals without adverse effects [30].

The degree of cooling appears to be limited to the proximity of the cooling site. Tanaka et al. cooled the hippocampus by a needle attached to a Peltier cell and measured a temperature reduction at the tip of the needle from 33.1 °C to 14.5 °C, but only below 25 °C in the 2.4 mm radius of the needle [21]. Similarly, we noted that 2.5 mm from the midline of the Peltier resulted

in only 3 °C and 1.5 °C temperature reduction at 0.5 A and 0.25 A, respectively. Interestingly, even at these farther sites with slight cooling a mitigation of epileptic activity was apparent.

One explanation for this could be the importance of cooling rate: spiking activity was reduced immediately after cooling onset, before reaching the maximum temperature drop at a given current strength - which took approximately 10 seconds - indicating that the speed of temperature reduction may be important besides reaching a particular threshold. Others made similar observations while cooling rat brain slices with artificial cerebrospinal fluid (aCSF) perfusion: rapid cooling by 1-2 °C aborts EDs, while complete termination of epileptic activity with slow cooling required temperature drops to 14-15 °C with 90% reduction in discharge frequency at 21-23 °C [35]. In this respect, Peltier cooling has the advantage over devices circulating liquid as a cooling medium that it is much faster. Using liquid cooling devices, depending on flow rate cooling to 20°C-27 °C required 3 minutes [16,17].

However, if a high enough rate of temperature reduction could cause diminished spiking, then it should have been apparent at the lowest driving current of 0.1 A, too. Because of this, we also hypothesize that the disruption of network synchrony caused by an effective degree of hypothermia [36] can spread to neighboring regions in the brain tissue that are not directly affected by cooling. This hypothesis needs further investigation.

The measurement setup combining a novel microECoG and Peltier cooling proved to be adequate to record electrophysiological signals from physiological and epileptic brain states, measure the surface temperature of the brain and exert local hypothermia to alter brain electrical activity. Steps towards clinical application of this concept would however require several modifications and future improvements. Ideally, the now separate units of the microECoG, cooling device and control board should be developed into one integrated system. This would radically improve the operation and usability of the device in a clinical scenario. One advantage of the custom microECoG design is that it is easily tailorable for human applications while retaining its current working principles. At the same time, difficulties are anticipated when scaling up the Peltier cooling: it would require larger external batteries to operate and solving heat dissipation needs would also be problematic. Therefore a cooling system with liquid circulation such as the one used by Smyth et al. [15] seems more appropriate for clinical applications. Also the recent advancements in seizure detection algorithms [37] show the potential of automatic initiation of cooling upon seizure occurrence. Seizure detection and prediction is also a key component in responsive neurostimulation (RNS), an alternative potential approach to refractory epilepsy treatment besides focal cooling [38,39]. RNS offers similar levels of specificity to focal cooling by implanting the stimulating electrode close to seizure onset zones, where electrical stimulation to

interrupt epileptic activity is applied acutely after seizure onset. With such device over the course of 9 years, a median reduction of 75% in seizures was reported [40].

There are numerous mechanisms through which hypothermia causes reduced neurologic functions: rapid reduction in neurotransmitter release [41], reversible disruption of the network synchrony [36], increased input resistance, decreased amplitude in population spikes and an increased spike duration [42–44], and reversible depolarization of the membrane potential [45,46] to name a few.

One way by which hypothermia may alter neural membrane properties is through its effect on ion channels. Changes in temperature affects all neurons and ion channels because channel gating is generally temperature-dependent [47]. However, there are only a very few ion channel types that can be designated as thermosensors [48].

Temperature sensitive cation channels may have an important role in hypothermia induced reduction of epileptic activity. Their two main categories are two-pore-domain potassium channels in the TREK and TRAAK family and the transient receptor potential (TRP) channels. Both can be activated by physiological temperatures, but they have opposing effects on neural excitability upon cooling.

Two-pore-domain potassium channels in the TREK and TRAAK family are expressed throughout the central nervous system. They are likely to help setting the resting membrane potential and neuronal input resistance because they are open at physiological membrane potentials, contributing to leak currents and opposing depolarizing influences [49,50]. Their open probability is high at 37 °C and it decreases dramatically at room temperature [51–53].

It is supposed that light to moderate cooling partially inactivates these channels leading to changes in firing rates as a network effect [54]. Mild cooling produces an increase in evoked and spontaneous synaptic activity in hippocampal slices that could be explained by the cold-induced closure of background TREK/TRAAK family channels [55].

Transient receptor potential (TRP) cationic channels can be activated by an increase or a drop in temperature, depending on their subtype [48]. Of the four subtypes activated by an increase in temperature, TRPV4 responds to the lowest of warm stimuli (>27 °C) [56] TRPV4 is a nonselective cation channel with high Ca^{2+} permeability [57] that is strongly expressed in the hippocampus activated by physiological brain temperatures thus enhancing brain activity, it has an important role in regulating neuronal excitability [58].

Deactivation of these channels by hypothermia has opposite effects in terms of neuronal excitability: closure of two-pore-domain channels increases evoked and spontaneous synaptic activity, while inhibition of TRPV4 reduces brain activity. With regards to epileptic seizures, the

net effect of cooling is suppressive suggesting a more pronounced role of TRPV4 deactivation. Indeed, TRPV4 may contribute to disease progression of epilepsy [59]. Epileptogenic foci possess elevated temperatures compared to healthy brain regions, and this activates TRPV4 channels. This was illustrated by wild type mice having greater epileptic EEG activity than TRPV4 knock-out mice [59].

On the other hand opening of TREK-1 by polyunsaturated fatty acids resulted in neuroprotection against ischemia and epilepsy. TREK-1 deficient mice show an increased sensitivity to these pathologies indicating a central role of TREK-1 in neuroprotection [49].

Although therapeutic hypothermia has promising qualities in reducing epileptic activity, it is already an established part of treatment for other diseases. Patients after cardiac arrest [60], infants with hypoxic ischemic encephalopathy [61] and severe traumatic brain injury (TBI) patients [62] may benefit from hypothermia treatment.

In future experiments, our toolset relying on a multimodal microECoG may provide substantial, novel information on neurophysiological processes in epileptic and other pathological states of the brain.

Acknowledgement

The authors are grateful for the funding of the National Development and Innovation Office (TKP2020-NKA-11 to Z.F., NKFIH FK 134403 to Z.F., NKFIH PD 134196 to R.F.) and the support of the Hungarian Brain Research Program (2017_1.2.1_NKP-2017-00002) and the National Bionics Research Program (ED_17_1_2017_0009 to A.P.). Support of the Hungarian Academy of Sciences through the Bolyai Fellowship to Z.F is also acknowledged.

References

1. Fisher, R.S.; Scharfman, H.E.; DeCurtis, M. How can we identify ictal and interictal abnormal activity? *Adv. Exp. Med. Biol.* **2014**, *813*, 3–23, doi:10.1007/978-94-17-8914-1_1.
2. Chabolla, D.R. Characteristics of the epilepsies. In Proceedings of the Mayo Clinic

Proceedings; Elsevier Ltd, 2002; Vol. 77, pp. 981–990.

3. Ko, D.Y. Epileptiform Discharges: Overview, Distinction From Normal or Nonspecific Sharp Transients, Localization and Clinical Significance of IEDs Available online: https://emedicine.medscape.com/article/1138880-overview (accessed on Mar 24, 2020).
4. Ramgopal, S.; Thome-Souza, S.; Jackson, M.; Kadish, N.E.; Sánchez Fernández, I.; Klehm, J.; Bosl, W.; Reinsberger, C.; Schachter, S.; Loddenkemper, T. Seizure detection, seizure prediction, and closed-loop warning systems in epilepsy. *Epilepsy Behav.* **2014**, *37*, 291–307, doi:10.1016/j.yebeh.2014.06.023.
5. Motamedi, G.K.; Lesser, R.P.; Vicini, S. Therapeutic brain hypothermia, its mechanisms of action, and its prospects as a treatment for epilepsy. *Epilepsia* **2013**, *54*, 959–970, doi:10.1111/epi.12144.
6. Fujii, M.; Fujioka, H.; Oku, T.; Tanaka, N.; Imoto, H.; Maruta, Y.; Nomura, S.; Kajiwara, K.; Saito, T.; Yamakawa, T.; et al. Application of focal cerebral cooling for the treatment of intractable epilepsy. *Neurol. Med. Chir. (Tokyo).* **2010**, *50*, 839–844, doi:10.2176/nmc.50.839.
7. Smyth, M.D.; Rothman, S.M. Focal Cooling Devices for the Surgical Treatment of Epilepsy. *Neurosurg. Clin. N. Am.* **2011**, *22*, 533–546, doi:10.1016/j.nec.2011.07.011.
8. Qiu, W.; Shen, H.; Zhang, Y.; Wang, W.; Liu, W.; Jiang, Q.; Luo, M.; Manou, M. Noninvasive selective brain cooling by head and neck cooling is protective in severe traumatic brain injury. *J. Clin. Neurosci.* **2006**, *13*, 995–1000, doi:10.1016/j.jocn.2006.02.027.
9. Linares, G.; Mayer, S.A. Hypothermia for the treatment of ischemic and hemorrhagic stroke. *Crit. Care Med.* **2009**, *37*, 243–249, doi:10.1097/CCM.0b013e3181aa5de1.
10. Karkar, K.M.; Garcia, P.A.; Bateman, L.M.; Smyth, M.D.; Barbaro, N.M.; Berger, M. Focal cooling suppresses spontaneous epileptiform activity without changing the cortical motor threshold. *Epilepsia* **2002**, *43*, 932–935, doi:10.1046/j.1528-1157.2002.03902.x.
11. Ablah, E.; Tran, M.P.; Isaac, M.; Kaufman, D.A.S.; Moufarrij, N.; Liow, K. Effect of cortical cooling on interictal epileptiform activities. *Seizure* **2009**, *18*, 61–63, doi:10.1016/j.seizure.2008.06.005.
12. Pásztor, E.; Tomka, I. Changes of electrocorticographic activity in response to direct brain surface cooling in epileptic patients. *Acta Physiol. Acad. Sci. Hung.* **1969**, *36*, 277–292.
13. Sartorius, C.J.; Berger, M.S. Rapid termination of intraoperative stimulation-evoked seizures with application of cold Ringer's lactate to the cortex. Technical note. *J.Neurosurg.* **1998**, *88*, 349–351.

14. D'Ambrosio, R.; Eastman, C.L.; Darvas, F.; Fender, J.S.; Verley, D.R.; Farin, F.M.; Wilkerson, H.W.; Temkin, N.R.; Miller, J.W.; Ojemann, J.; et al. Mild passive focal cooling prevents epileptic seizures after head injury in rats. *Ann. Neurol.* **2013**, *73*, 199–209, doi:10.1002/ana.23764.
15. Smyth, M.D.; Han, R.H.; Yarbrough, C.K.; Patterson, E.E.; Yang, X.-F.; Miller, J.W.; Rothman, S.M.; D'Ambrosio, R. Temperatures Achieved in Human and Canine Neocortex During Intraoperative Passive or Active Focal Cooling. *Ther. Hypothermia Temp. Manag.* **2015**, *5*, 95–103, doi:10.1089/ther.2014.0025.
16. Burton, J.M.; Peebles, G.A.; Binder, D.K.; Rothman, S.M.; Smyth, M.D. Transcortical cooling inhibits hippocampal-kindled seizures in the rat. *Epilepsia* **2005**, *46*, 1881–1887, doi:10.1111/j.1528-1167.2005.00299.x.
17. Cooke, D.F.; Goldring, A.B.; Yamayoshi, I.; Tsourkas, P.; Recanzone, G.H.; Tiriac, A.; Pan, T.; Simon, S.I.; Krubitzer, L. Fabrication of an inexpensive, implantable cooling device for reversible brain deactivation in animals ranging from rodents to primates. *J. Neurophysiol.* **2012**, *107*, 3543–3558, doi:10.1152/jn.01101.2011.
18. Nomura, S.; Inoue, T.; Imoto, H.; Suehiro, E.; Maruta, Y.; Hirayama, Y.; Suzuki, M. Effects of focal brain cooling on extracellular concentrations of neurotransmitters in patients with epilepsy. *Epilepsia* **2017**, *58*, 627–634, doi:10.1111/epi.13704.
19. Nomura, S.; Fujii, M.; Inoue, T.; He, Y.; Maruta, Y.; Koizumi, H.; Suehiro, E.; Imoto, H.; Ishihara, H.; Oka, F.; et al. Changes in glutamate concentration, glucose metabolism, and cerebral blood flow during focal brain cooling of the epileptogenic cortex in humans. *Epilepsia* **2014**, *55*, 770–776, doi:10.1111/epi.12600.
20. Kida, H.; Fujii, M.; Inoue, T.; He, Y.; Maruta, Y.; Nomura, S.; Taniguchi, K.; Ichikawa, T.; Saito, T.; Yamakawa, T.; et al. Focal brain cooling terminates the faster frequency components of epileptic discharges induced by penicillin G in anesthetized rats. *Clin. Neurophysiol.* **2012**, *123*, 1708–1713, doi:10.1016/j.clinph.2012.02.074.
21. Tanaka, N.; Fujii, M.; Imoto, H.; Uchiyama, J.; Nakano, K.; Nomura, S.; Fujisawa, H.; Kunitsugu, I.; Saito, T.; Suzuki, M. Effective suppression of hippocampal seizures in rats by direct hippocampal cooling with a Peltier chip. *J. Neurosurg.* **2008**, *108*, 791–797, doi:10.3171/jns/2008/108/4/0791.
22. Rubehn, B.; Bosman, C.; Oostenveld, R.; Fries, P.; Stieglitz, T. A MEMS-based flexible multichannel ECoG-electrode array. *J. Neural Eng.* **2009**, *6*, 036003, doi:10.1088/1741-2560/6/3/036003.
23. Zátonyi, A.; Fedor, F.; Borhegyi, Z.; Fekete, Z. In vitro and in vivo stability of black-

platinum coatings on flexible, polymer microECoG arrays. *J. Neural Eng.* **2018**, *15*, 054003, doi:10.1088/1741-2552/aacf71.

24. Zátonyi, A.; Borhegyi, Z.; Srivastava, M.; Cserpán, D.; Somogyvári, Z.; Kisvárday, Z.; Fekete, Z. Functional brain mapping using optical imaging of intrinsic signals and simultaneous high-resolution cortical electrophysiology with a flexible, transparent microelectrode array. *Sensors Actuators, B Chem.* **2018**, *273*, 519–526, doi:10.1016/j.snb.2018.06.092.
25. Fedor, F.Z.; Zátonyi, A.; Cserpán, D.; Somogyvári, Z.; Borhegyi, Z.; Juhász, G.; Fekete, Z. Application of a flexible polymer microECoG array to map functional coherence in schizophrenia model. *MethodsX* **2020**, *7*, doi:10.1016/j.mex.2020.101117.
26. Rubehn, B.; Stieglitz, T. In vitro evaluation of the long-term stability of polyimide as a material for neural implants. *Biomaterials* **2010**, *31*, 3449–3458, doi:10.1016/j.biomaterials.2010.01.053.
27. Leber, M.; Bhandari, R.; Mize, J.; Warren, D.J.; Shandhi, M.M.H.; Solzbacher, F.; Negi, S. Long term performance of porous platinum coated neural electrodes. *Biomed. Microdevices* **2017**, *19*, 1–12, doi:10.1007/s10544-017-0201-4.
28. Fujii, M.; Inoue, T.; Nomura, S.; Maruta, Y.; He, Y.; Koizumi, H.; Shirao, S.; Owada, Y.; Kunitsugu, I.; Yamakawa, T.; et al. Cooling of the epileptic focus suppresses seizures with minimal influence on neurologic functions. *Epilepsia* **2012**, *53*, 485–493, doi:10.1111/j.1528-1167.2011.03388.x.
29. Oku, T.; Fujii, M.; Tanaka, N.; Imoto, H.; Uchiyama, J.; Oka, F.; Kunitsugu, I.; Fujioka, H.; Nomura, S.; Kajiwara, K.; et al. The influence of focal brain cooling on neurophysiopathology: validation for clinical application. *J. Neurosurg.* **2009**, *110*, 1209–1217, doi:10.3171/2009.1.jns08499.
30. Kowski, A.B.; Kanaan, H.; Schmitt, F.C.; Holtkamp, M. Deep hypothermia terminates status epilepticus - An experimental study. *Brain Res.* **2012**, *1446*, 119–126, doi:10.1016/j.brainres.2012.01.022.
31. Nomura, S.; Kida, H.; Hirayama, Y.; Imoto, H.; Inoue, T.; Moriyama, H.; Mitsushima, D.; Suzuki, M. Reduction of spike generation frequency by cooling in brain slices from rats and from patients with epilepsy. *J. Cereb. Blood Flow Metab.* **2019**, *39*, 2286–2294, doi:10.1177/0271678X18795365.
32. Yang, X.F.; Duffy, D.W.; Morley, R.E.; Rothman, S.M. Neocortical seizure termination by focal cooling: Temperature dependence and automated seizure detection. *Epilepsia* **2002**, *43*, 240–245, doi:10.1046/j.1528-1157.2002.33301.x.

33. Yang, X.F.; Rothman, S.M. Focal cooling rapidly terminates experimental neocortical seizures. *Ann. Neurol.* **2001**, *49*, 721–726, doi:10.1002/ana.1021.
34. Hill, M.W.; Wong, M.; Amarakone, A.; Rothman, S.M. Rapid cooling aborts seizure-like activity in rodent hippocampal-entorhinal slices. *Epilepsia* **2000**, *41*, 1241–1248, doi:10.1111/j.1528-1157.2000.tb04601.x.
35. Motamedi, G.K.; Salazar, P.; Smith, E.L.; Lesser, R.P.; Webber, W.R.S.; Ortinski, P.I.; Vicini, S.; Rogawski, M.A. Termination of epileptiform activity by cooling in rat hippocampal slice epilepsy models. *Epilepsy Res.* **2006**, *70*, 200–210, doi:10.1016/j.eplepsyres.2006.05.001.
36. Rossetti, A.O.; Lowenstein, D.H. Management of refractory status epilepticus in adults: Still more questions than answers. *Lancet Neurol.* **2011**, *10*, 922–930, doi:10.1016/S1474-4422(11)70187-9.
37. Göksu, H. EEG based epileptiform pattern recognition inside and outside the seizure states. *Biomed. Signal Process. Control* **2018**, *43*, 204–215, doi:10.1016/j.bspc.2018.03.004.
38. Morrell, M. Brain stimulation for epilepsy: Can scheduled or responsive neurostimulation stop seizures? *Curr. Opin. Neurol.* **2006**, *19*, 164–168, doi:10.1097/01.wco.0000218233.60217.84.
39. Sun, F.T.; Morrell, M.J.; Wharen, R.E. Responsive Cortical Stimulation for the Treatment of Epilepsy. *Neurotherapeutics* **2008**, *5*, 68–74, doi:10.1016/j.nurt.2007.10.069.
40. Skarpaas, T.L.; Jarosiewicz, B.; Morrell, M.J. Brain-responsive neurostimulation for epilepsy (RNS ® System). *Epilepsy Res.* **2019**, *153*, 68–70, doi:10.1016/j.eplepsyres.2019.02.003.
41. Yang, X.F.; Ouyang, Y.; Kennedy, B.R.; Rothman, S.M. Cooling blocks rat hippocampal neurotransmission by a presynaptic mechanism: Observation using 2-photon microscopy. *J. Physiol.* **2005**, *567*, 215–224, doi:10.1113/jphysiol.2005.088948.
42. Andersen, P.; Gjerstad, L.; Pasztor, E. Effects of Cooling on Inhibitory Processes in the Cuneate Nucleus. *Acta Physiol. Scand.* **1972**, *84*, 448–461, doi:10.1111/j.1748-1716.1972.tb05195.x.
43. Andersen, P.; Gjerstad, L.; Pasztor, E. Effect of cooling on synaptic transmission through the cuneate nucleus. *Acta Physiol. Scand.* **1972**, *84*, 433–447, doi:10.1111/j.1748-1716.1972.tb05194.x.
44. Shen, K.F.; Schwartzkroin, P.A. Effects of temperature alterations on population and cellular activities in hippocampal slices from mature and immature rabbit. *Brain Res.*

1988, *475*, 305–316, doi:10.1016/0006-8993(88)90619-1.

45. Thompson, S.M.; Masukawa, L.M.; Prince, D.A. Temperature dependence of intrinsic membrane properties and synaptic potentials in hippocampal CA1 neurons in vitro. *J. Neurosci.* **1985**, *5*, 817–824.
46. Volgushev, M.; Vidyasagar, T.R.; Chistiakova, M.; Yousef, T.; Eysel, U.T. Membrane properties and spike generation in rat visual cortical cells during reversible cooling. *J. Physiol.* **2000**, *522*, 59–76, doi:10.1111/j.1469-7793.2000.0059m.x.
47. Brauchi, S.; Orio, P.; Latorre, R. Clues to understanding cold sensation: Thermodynamics and electrophysiological analysis of the cold receptor TRPM8. *Proc. Natl. Acad. Sci. U. S. A.* **2004**, *101*, 15494–15499, doi:10.1073/pnas.0406773101.
48. Lamas, J.A.; Rueda-Ruzafa, L.; Herrera-Pérez, S. Ion Channels and Thermosensitivity: TRP, TREK, or Both? *Int. J. Mol. Sci.* **2019**, *20*, 2371, doi:10.3390/ijms20102371.
49. Heurteaux, C.; Guy, N.; Laigle, C.; Blondeau, N.; Duprat, F.; Mazzuca, M.; Lang-Lazdunski, L.; Widmann, C.; Zanzouri, M.; Romey, G.; et al. TREK-1, a K+ channel involved in neuroprotection and general anesthesia. *EMBO J.* **2004**, *23*, 2684–2695, doi:10.1038/sj.emboj.7600234.
50. Lesage, F. Pharmacology of neuronal background potassium channels. *Neuropharmacology* **2003**, *44*, 1–7, doi:10.1016/S0028-3908(02)00339-8.
51. Maingret, F.; Lauritzen, I.; Patel, A.J.; Heurteaux, C.; Reyes, R.; Lesage, F.; Lazdunski, M.; Honoré, E. TREK-1 is a heat-activated background K+ channel. *EMBO J.* **2000**, *19*, 2483–2491, doi:10.1093/emboj/19.11.2483.
52. Schneider, E.R.; Anderson, E.O.; Gracheva, E.O.; Bagriantsev, S.N. Temperature Sensitivity of Two-Pore (K2P) Potassium Channels. *Curr. Top. Membr.* **2014**, *74*, 113–133, doi:10.1016/B978-0-12-800181-3.00005-1.
53. Kang, D.; Choe, C.; Kim, D. Thermosensitivity of the two-pore domain K+ channels TREK-2 and TRAAK. *J. Physiol.* **2005**, *564*, 103–116, doi:10.1113/jphysiol.2004.081059.
54. Burkhanova, G.; Chernova, K.; Khazipov, R.; Sheroziya, M. Effects of Cortical Cooling on Activity Across Layers of the Rat Barrel Cortex. *Front. Syst. Neurosci.* **2020**, *14*, doi:10.3389/fnsys.2020.00052.
55. de la Peña, E.; Mälkiä, A.; Vara, H.; Caires, R.; Ballesta, J.J.; Belmonte, C.; Viana, F. The Influence of Cold Temperature on Cellular Excitability of Hippocampal Networks. *PLoS One* **2012**, *7*, doi:10.1371/journal.pone.0052475.
56. Dhaka, A.; Viswanath, V.; Patapoutian, A. TRP ion channels and temperature sensation. *Annu. Rev. Neurosci.* **2006**, *29*, 135–161, doi:10.1146/annurev.neuro.29.051605.112958.

57. Shibasaki, K. TRPV4 activation by thermal and mechanical stimuli in disease progression. *Lab. Investig.* **2020**, *100*, 218–223, doi:10.1038/s41374-019-0362-2.
58. Shibasaki, K.; Suzuki, M.; Mizuno, A.; Tominaga, M. Effects of body temperature on neural activity in the hippocampus: Regulation of resting membrane potentials by transient receptor potential vanilloid 4. *J. Neurosci.* **2007**, *27*, 1566–1575, doi:10.1523/JNEUROSCI.4284-06.2007.
59. Shibasaki, K.; Yamada, K.; Miwa, H.; Yanagawa, Y.; Suzuki, M.; Tominaga, M.; Ishizaki, Y. Temperature elevation in epileptogenic foci exacerbates epileptic discharge through TRPV4 activation. *Lab. Investig.* **2020**, *100*, 274–284, doi:10.1038/s41374-019-0335-5.
60. Bernard, S.A.; Gray, T.W.; Buist, M.D.; Jones, B.M.; Silvester, W.; Gutteridge, G.; Smith, K. Treatment of Comatose Survivors of Out-of-Hospital Cardiac Arrest with Induced Hypothermia. *N. Engl. J. Med.* **2002**, *346*, 557–563, doi:10.1056/NEJMoa003289.
61. Shankaran, S.; Laptook, A.R.; Ehrenkranz, R.A.; Tyson, J.E.; McDonald, S.A.; Donovan, E.F.; Fanaroff, A.A.; Poole, W.K.; Wright, L.L.; Higgins, R.D.; et al. Whole-Body Hypothermia for Neonates with Hypoxic–Ischemic Encephalopathy. *N. Engl. J. Med.* **2005**, *353*, 1574–1584, doi:10.1056/nejmcps050929.
62. Marion, D.W.; Penrod, L.E.; Kelsey, S.F.; Obrist, W.D.; Kochanek, P.M.; Palmer, A.M.; Wisniewski, S.R.; DeKosky, S.T. Treatment of Traumatic Brain Injury with Moderate Hypothermia. *N. Engl. J. Med.* **1997**, *336*, 540–546, doi:10.1056/nejm199702203360803.
63. González-Ibarra, F.P.; Varon, J.; López-Meza, E.G. Therapeutic hypothermia: Critical review of the molecular mechanisms of action. *Front. Neurol.* **2011**, *2*, doi:10.3389/fneur.2011.00004.
64. Kimura, A.; Sakurada, S.; Ohkuni, H.; Todome, Y.; Kurata, K. Moderate hypothermia delays proinflammatory cytokine production of human peripheral blood mononuclear cells. *Crit. Care Med.* **2002**, *30*, 1499–1502, doi:10.1097/00003246-200207000-00017.
65. Xiong, M.; Yang, Y.; Chen, G.-Q.; Zhou, W.-H. Post-ischemic hypothermia for 24h in P7 rats rescues hippocampal neuron: Association with decreased astrocyte activation and inflammatory cytokine expression. *Brain Res. Bull.* **2009**, *79*, 351–357, doi:10.1016/j.brainresbull.2009.03.011.
66. Polderman, K.H. Mechanisms of action, physiological effects, and complications of hypothermia. *Crit. Care Med.* **2009**, *37*, 186–202, doi:10.1097/CCM.0b013e3181aa5241.
67. Chieko Okuda; Akiko Saito; Masao Miyazaki; Kinya Kuriyama Alteration of the turnover of dopamine and 5-hydroxytryptamine in rat brain associated with hypothermia. *Pharmacol. Biochem. Behav.* **1986**, *24*, 79–83, doi:10.1016/0091-3057(86)90048-1.

Figure captions

Figure 1. Layout of the multimodal microECoG array with 32 electrical recording sites (red dots) and 8 temperature sensors in a 3-2-3 configuration between them (A). The blue rectangle represents the footprint of the Peltier chip. An integrated temperature sensor (B) and a recording site (C) is shown in more details. A cross-sectional schematic (D) shows the layer structure in planes aa' and bb'. Plane aa' contains four platinum recording sites, and plane bb' goes through two platinum temperature sensors and an aperture between them dedicated for syringe insertion. (E) The ready-to-use microECoG array. (F) Close view on the 32 recording sites and 8 temperature sensors. Scale bars in panels E-F show 8 mm, 0.3 mm, respectively. All dimensions on panels A-C are in mm.

Figure 2. Photo of the core component of the cooling actuator (A) and a schematic (B) showing the arrangement during *in vivo* experiments. The exposed brain tissue (1) is covered by the multimodal microECoG device (2). After bicuculline injection, the Peltier chip (3) already fixed on the heat-pipe (4) with conductive glue was placed on top of the microECoG. Photo (C) shows the final cooling procedure after drug administration.

Figure 3. Long-term electrochemical performance of the proposed material composition. Bode plot on the first (A) and 22nd (B) day of the electrochemical stability experiment. Pale lines represent the unique curves of each recording site (n = 32), dark lines represent mean curves of impedance (black) and phase (blue). (C) Mean impedance values ± standard deviation of 32 recording sites at 1 kHz during the soaking period (22 days). (D) Changes in surface temperature on agarose gel during the calibration process using various driving currents. Underneath the chip, a strong cooling effect can be monitored through the integrated temperature sensors, which drops quickly moving away from the chip outline.

Figure 4. Change in temperature at some distances from the midline of the Peltier chip using the agar gel model with driving currents (A) 0.1 A, (B) 0.25 A and (C) 0.5 A.

Figure 5. (A) One-minute-long raw data from all 32 channels before, during and after cooling the cortical surface (I = 0.1 A). (B) One-minute-long raw data from all 32 channels before, during and after cooling the cortical surface (I = 0.25 A). (C) One-minute-long raw data from all 32 channels before, during and after cooling the cortical surface (I = 0.5 A). Changes in the frequency and

amplitude of ictal spikes are notable. During cooling the dimensions of the Peltier chip are represented by a blue background, and the injection area with red background behind the graphs of the channels.

Figure 6. Representative recordings on a single channel next to the Peltier chip showing the effect of cortical cooling on ictal spiking activity at the initial state of ictal activity (A-C) and at an advanced state (D). (A) I = 0.1 A, (B) I = 0.25 A (C) I = 0.5 A, (D) I = 0.5 A. The subsequent one-minute-long traces are composed of cooling OFF (red background) and cooling ON (blue background) states. (D) also demonstrates the longevity of spike rate suppression during a five-minute-long cooling phase. The cooling with 0.1 A has no significant effect on the spike rate.

Figure 7. Effect of cooling on spike rate and average amplitude baseline before cooling, during cooling (for 5 minutes) and baseline after cooling. (A) Spike rates I = 0.25 A, (B) Spike rates I = 0.5 A, (C) Average amplitude I = 0.25 A, (D) Average amplitude I = 0.5 A. The color of the box indicates the baseline (red) and the cooling (blue)

Figures

Figure 1.

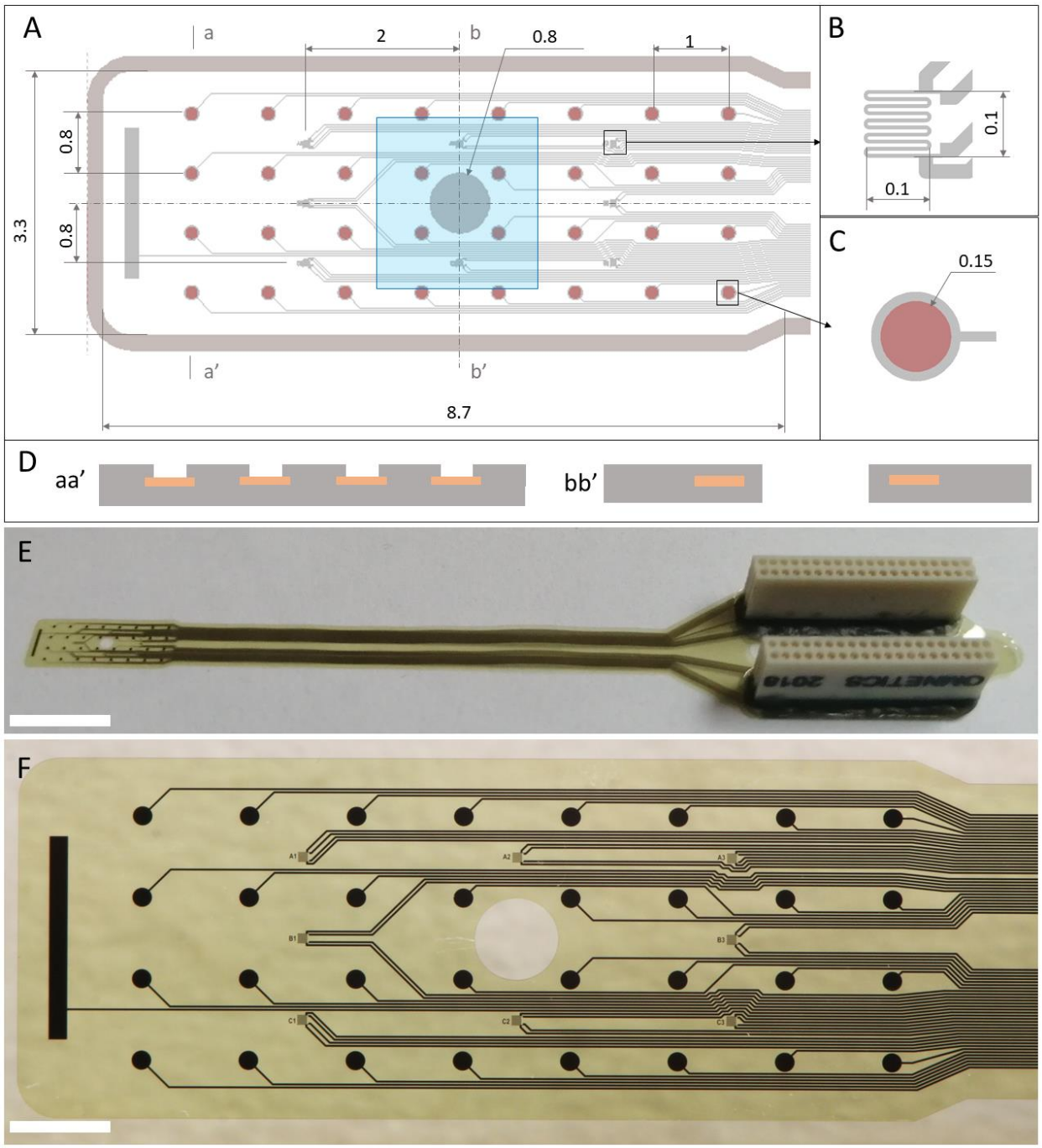

Figure 2.

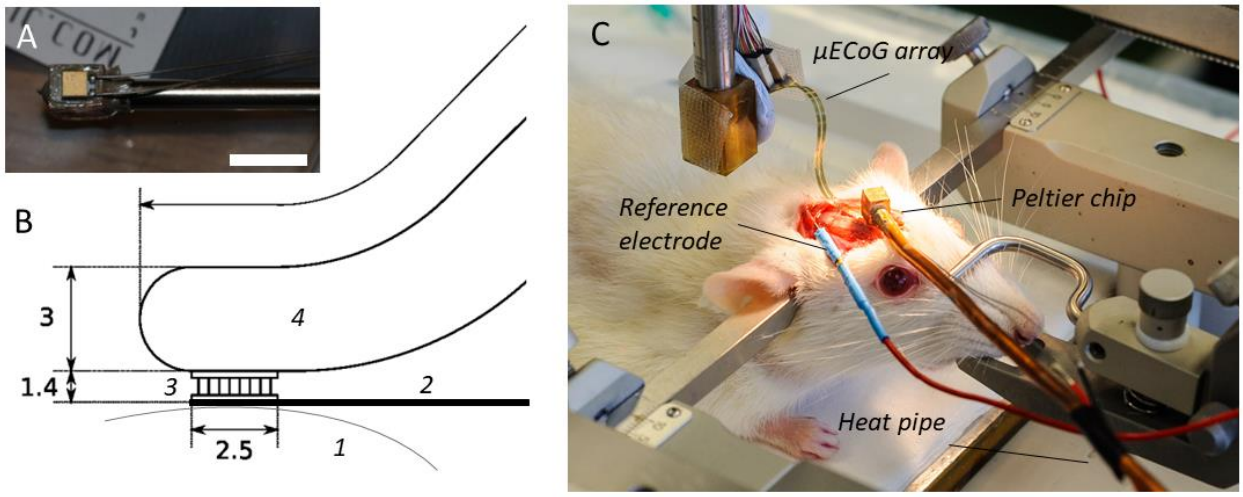
A
B
3
1.4
4
3
2
2.5
1
C
μECoG array
Reference electrode
Peltier chip
Heat pipe

Figure 3.

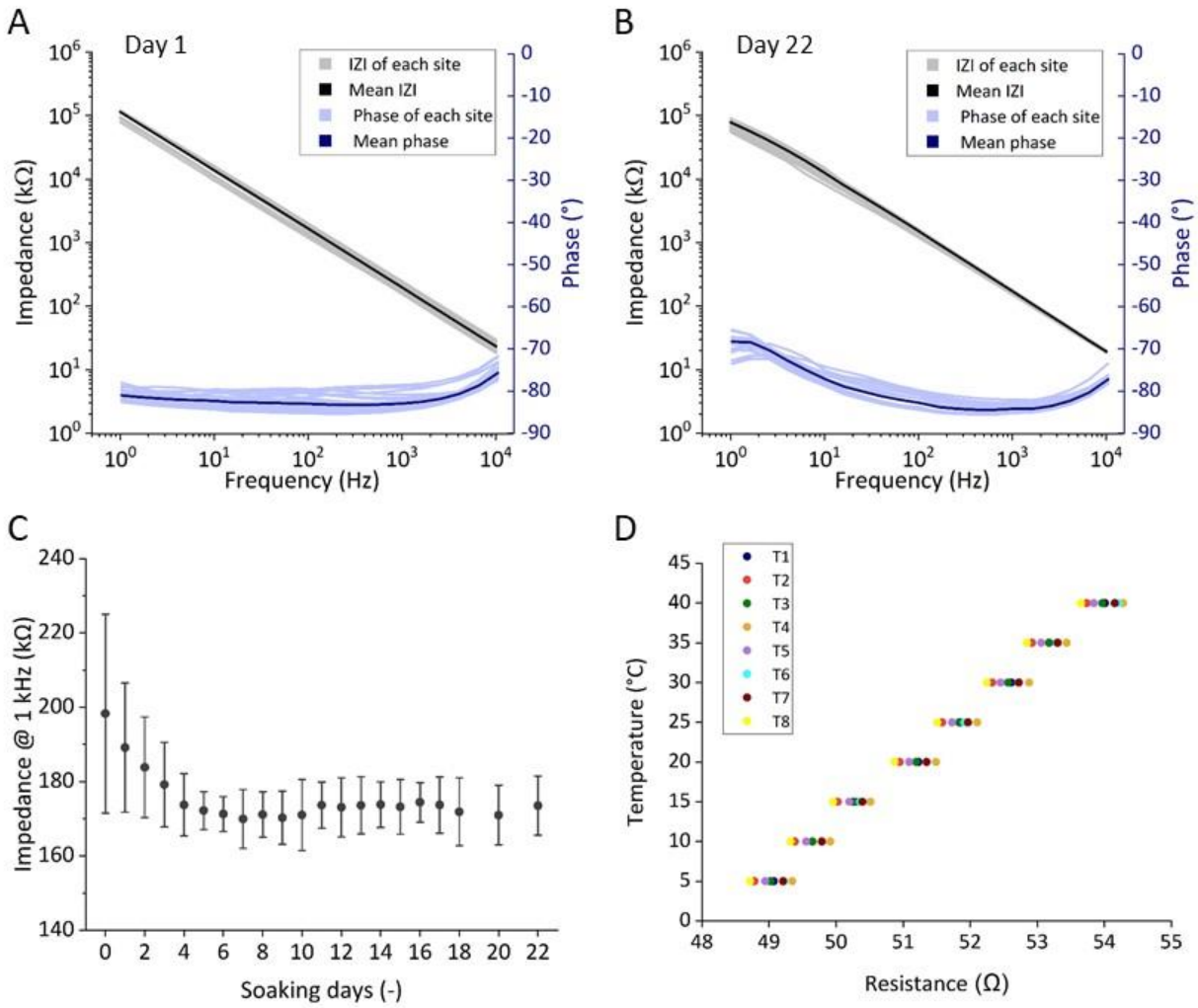
A
Day 1
IZI of each site
Mean IZI
Phase of each site
Mean phase
Impedance (kΩ)
Phase (°)
Frequency (Hz)
B
Day 22
IZI of each site
Mean IZI
Phase of each site
Mean phase
Impedance (kΩ)
Phase (°)
Frequency (Hz)
C
Impedance @ 1 kHz (kΩ)
Soaking days (-)
D
T1
T2
T3
T4
T5
T6
T7
T8
Temperature (°C)
Resistance (Ω)

Figure 4.

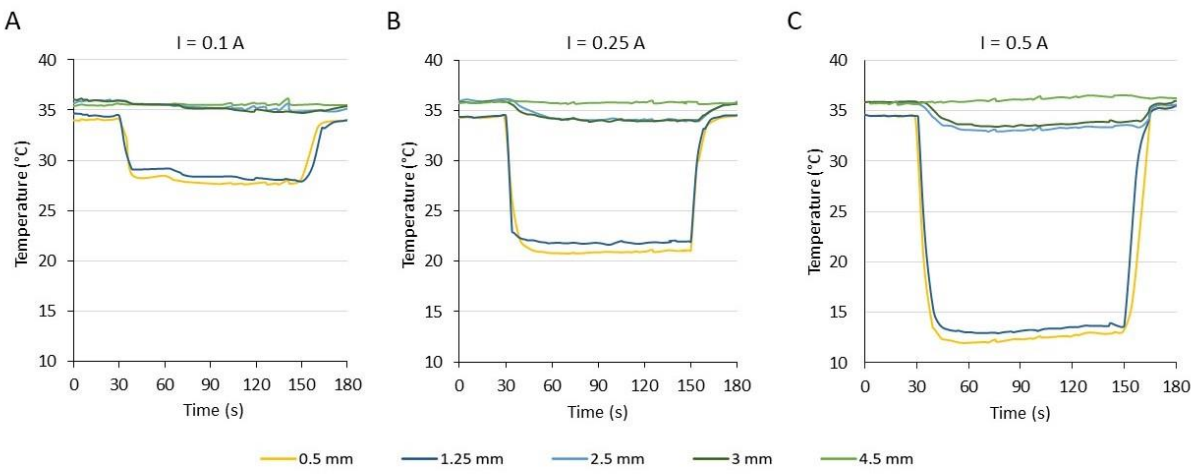
A
I = 0.1 A
B
I = 0.25 A
C
I = 0.5 A
Temperature (°C)
Time (s)
0.5 mm
1.25 mm
2.5 mm
3 mm
4.5 mm

Figure 5.

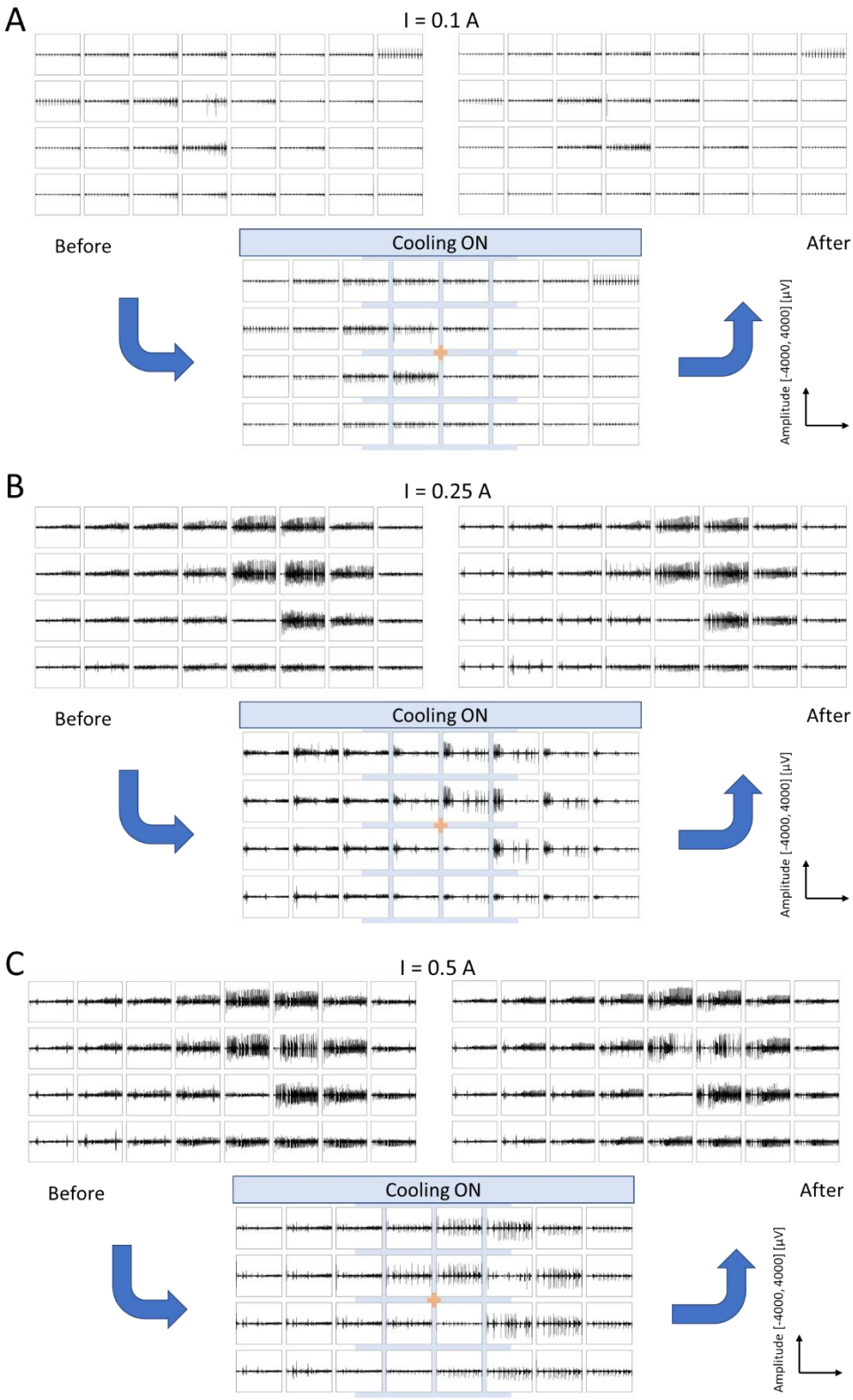
A
I = 0.1 A
Before
Cooling ON
After
Amplitude [-4000, 4000] [µV]
B
I = 0.25 A
Before
Cooling ON
After
Amplitude [-4000, 4000] [µV]
C
I = 0.5 A
Before
Cooling ON
After
Amplitude [-4000, 4000] [µV]

Figure 6.

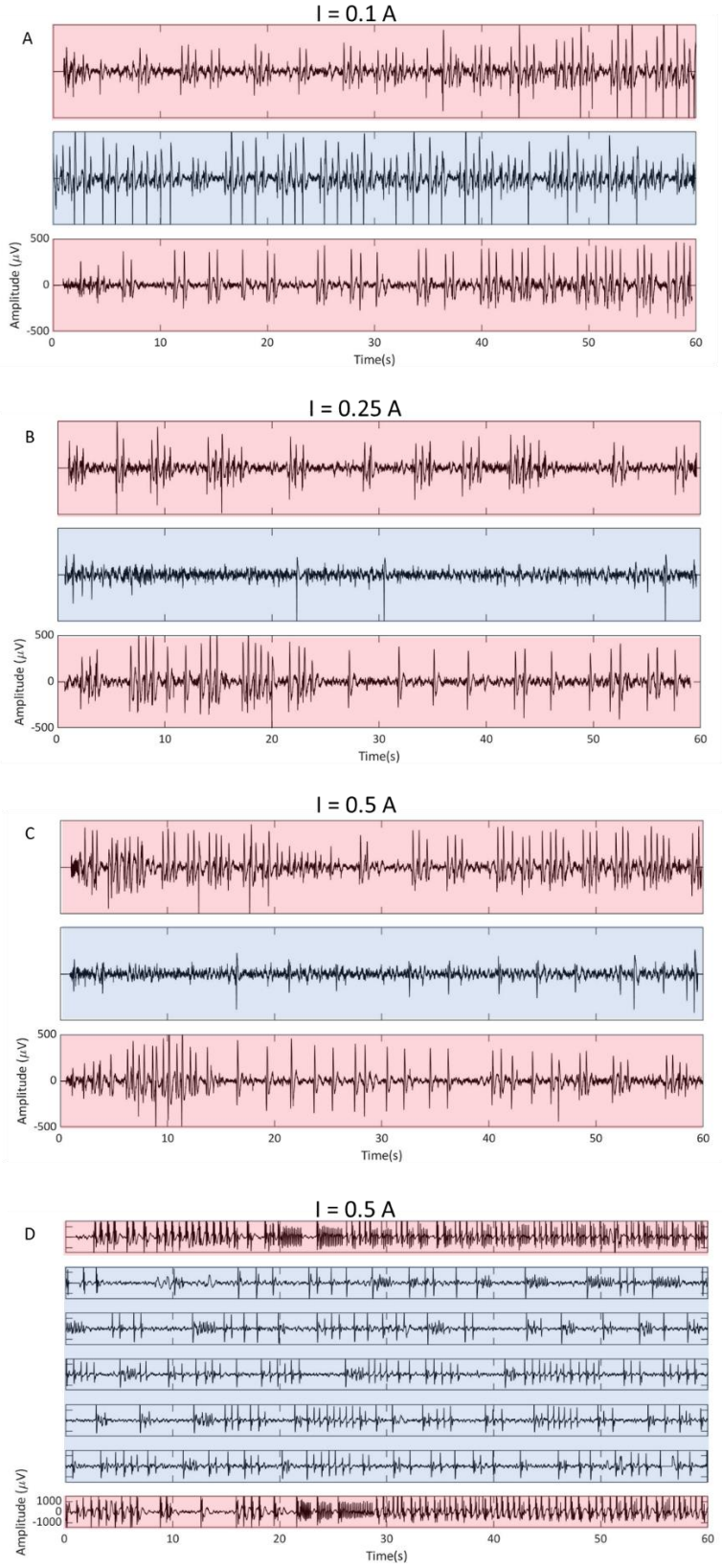
I = 0.1 A
A
Amplitude (μV)
500
0
-500
0
10
20
30
40
50
60
Time(s)
I = 0.25 A
B
Amplitude (μV)
500
0
-500
0
10
20
30
40
50
60
Time(s)
I = 0.5 A
C
Amplitude (μV)
500
0
-500
0
10
20
30
40
50
60
Time(s)
I = 0.5 A
D
Amplitude (μV)
1000
0
-1000
0
10
20
30
40
50
60
Time(s)

Figure 7.

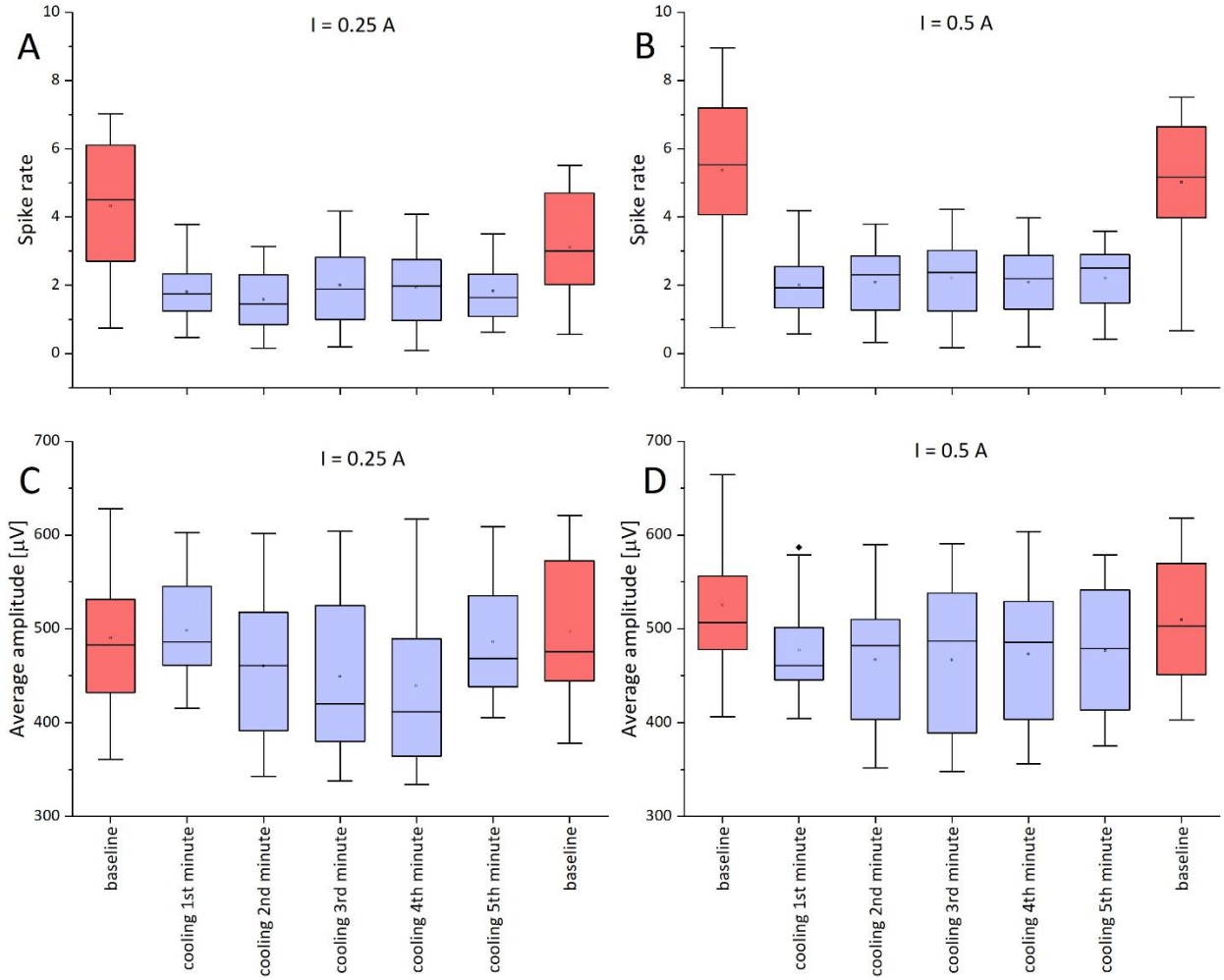
A
I = 0.25 A
Spike rate
B
I = 0.5 A
Spike rate
C
I = 0.25 A
Average amplitude [µV]
D
I = 0.5 A
Average amplitude [µV]
baseline
cooling 1st minute
cooling 2nd minute
cooling 3rd minute
cooling 4th minute
cooling 5th minute
baseline